Supplementary Materials

S1 - Additional information on participants demographics and psychiatric comorbidities

Participants were recruited and assessed at three sites: (1) The Institute of Psychiatry, Psychology and Neuroscience (IoPPN), London, UK (n=39, including 25 individuals with 22q11.2DS and 14 controls); (2) the Semel Institute for Neuroscience and Human Behaviour, University of California (UCLA), Los Angeles, US (n=39, including 25 individuals with 22q11.2DS and 14 controls); and (3) the Department of Child and Adolescent Psychiatry, University Hospital Frankfurt, Goethe University (GU) Frankfurt, Germany (n=53, including 40 individuals with idiopathic ASD and 13 controls).

In the idiopathic ASD group, 2 females differed slightly from the inclusion criteria for ASD. However, due to few female datasets being available to us, we decided to include these to ensure gender balanced groups. One female scored above the cutoff in the reciprocal social interaction domain and restricted and repetitive behaviours domain but fell short in the communication domain. For another, we were unable to obtain ADI-R information, however, this individual scored well above the threshold on the calibrated severity score of the ADOS (8 out of 10) (Gotham K et al. 2009; Hus V et al. 2014).

Exclusion criteria for all participants included a full-scale IQ below 60. Further exclusion criteria for all participants included contraindications to MRI and any medical condition or chromosomal anomaly other than 22q11.2DS, which may be associated with ASD or psychosis (e.g. tuberous sclerosis, Fragile X syndrome or Prader-Willi syndrome). 22q11.2DS individuals with psychiatric co-morbidities (i.e. schizophrenia, bipolar, psychosis etc) were included, as these are common co-morbid features of the microdeletion. In the current sample, however, only one participant (in the 22q11.ASD group) had a diagnosis of previous episode of schizophrenia, with no symptoms at the time of assessment. Attention hyperactivity disorder (ADHD) and neuropsychiatric disorders (e.g. anxiety, depression) were allowed in all groups. For all participants assessed at the IoPPN and at UCLA, psychiatric comorbidities were determined by the Structured Clinical Interview for DSM-IV (SCID) for those over 18 (First MB and M Gibbon 2004), and the Computerized Diagnostic Interview Schedule for Children (C-DISC; based on DSM-IV) for those under 18 (Shaffer D et al. 1993). For all participants assessed in Frankfurt, a comorbid diagnosis of ADHD and Oppositional Defiance Disorder (ODD) was determined by the Diagnostic System for Mental Disorders According to ICD-10 and DSM-IV for children and adolescents-II (DISYPS-II) (Döpfner M et al. 2008). Please also see

Table S2 below for a summary of psychiatric diagnoses. Further, to assess prodromal symptoms of psychosis in our sample, we administered the Structured Interview for prodromal syndromes (SIPS) (McGlashan TH 2001) in all our participants with 22q11.2DS (see Table S3 for details).

S2 – Psychiatric co-morbidities across group

	22q11.nonASD (n = 25)	22q11.ASD (n = 25)	ASD (n = 40)	Controls (n = 41)
Depression	0	3	1	0
ADHD	7	8	14	3
Panic Disorder	1	1	0	0
ODD	3	2	0	0
Social Phobia	1	4	0	0
GAD	0	4	0	0
Separation Anxiety	0	1	0	0

Note: ADHD; Attention Hyperactivity Disorder, ODD; Oppositional defiant disorder, GAD; Generalized Anxiety Disorder.

There were no significant differences between the 22q11.2DS group and the non22q11.2 group in frequency of comorbid diagnoses of ADHD and depression (x^2=2.900, p=0.089, and x^2=2.372, p=0.124 respectively). All other psychiatric co-morbidities were only present in the non22q11.2DS individuals, as these were among the exclusion criteria for idiopathic ASD and TD Controls.

S3 – SIPS scores across 22q11.2DS individuals

	22q11.nonASD (n = 21)		22q11.ASD (n = 18)		Test Statistic	
					t	*p*
SIPS Positive Symptoms	4 ± 4	(0-13)	3 ± 3	(0-15)	-0.770	0.446
SIPS Negative Symptoms	4 ± 4	(0-11)	5 ± 4	(0-16)	1.014	0.317

Note: SIPS; Structured Interview for prodromal syndromes.

S4 - Quality Assessments and Manual Edits

For each scan, the FreeSurfer derived surface models were visually inspected for reconstruction errors, and quality was rated based on the following three options: (1) accept as is (no visible reconstruction errors or artefacts), (2) prescribe manual edits (visible reconstruction errors in either pial or white matter surface (or both) that might be recoverable using manual edits), or (3) exclude (gross anatomical abnormalities or severe acquisition artifacts). Manual edits were performed by making changes to the pial (i.e. grey matter) outline, to the white matter outline, or both. Following manual editing, images were (re-)preprocessed and re-assessed for reconstruction errors. Further details on quality assessments and scan exclusion rates are described in (Gudbrandsen M et al. 2019) for scans acquired at the IoPPN and UCLA. The scans acquired in Frankfurt were selected from a larger ongoing study based on participant's age, gender, and IQ. Here, quality assessments and manual edits were conducted using the same stringent criteria as outlined above.

S5 - Additional information on Canonical Correlation Analysis (CCA)

In brief, CCA aims to describe the linear relationship between a set of *n* x *p* predictor variables (X) and *n* x *q* outcome measures (Y), where *n* indicates the number of participants. Initially, CCA estimates two parameter vectors α and β so that the correlation ρ between the linear combinations $\hat{X} = \alpha^T X$ and $\hat{Y} = \beta^T Y$ is maximised, i.e.

$$\rho = \text{corr}(\hat{X}, \hat{Y}) = \max_{\alpha,\beta} \text{corr}(\alpha^T X, \beta^T Y)$$

The resulting predicted variables $\hat{X}1$ and $\hat{Y}1$ are the first pair of canonical variates (CV), and their correlation ρ1 is the first canonical correlation (CC). Similar to Principle Component Analysis (PCA), the second set of parameter estimates maximizing ρ is then derived subject to the constraint of being uncorrelated with the first pair of canonical variates. This procedure may be continued up to i times, where i = min{p, q}, resulting in maximally i canonical variate pairs. The R-square type (ρ^2) effect size of the reported model represents a 'volumetric' measure of multivariate association and indicates the percentage of shared variance between both data modalities. It is computed as (1 – Wilk's Lambda) across CVs, where Wilk's Lambda is a product of the values (1 – canonical correlations^2) across the *i* canonical correlations. It is important to note that CVs are 'derived' or 'latent' variables that are estimated to maximize the correlation between *X* and *Y*. It is therefore crucial to also examine the statistical significance of each individual component based on the percentage of 'explained' rather than 'shared' variance. Here, we also explored the percentage of variance explained by each CV and tested for their statistical significance using Wilks' λ and Bartlett's Chi-squared test (Snedecor and Cochran 1989). Only CVs that explained sufficient clinical variance were retained for further analysis.

CCA was initially applied to the non22q11.2DS individuals to establish the relationship between neuroanatomical variability and inter-individual differences in autistic symptom profiles. The same canonical model was then fitted to individuals with the 22q11.2 microdeletion. To compare results across groups, two different visual representations were utilised: (1) canonical loading (λ_C) plots based on the individuals features spanning X and Y, which represent the correlations between each

feature and the respective canonical variates (i.e. $r(x_{1...n}, \hat{X}_i)$ or $r(y_{1...n}, \hat{Y}_i)$), and (2) scatter plots of the individual observations (i.e. cases) based on their canonical variate scores (i.e. $\hat{X}_i$ or $\hat{Y}_i$).

S6 - Canonical Correlation Diagram

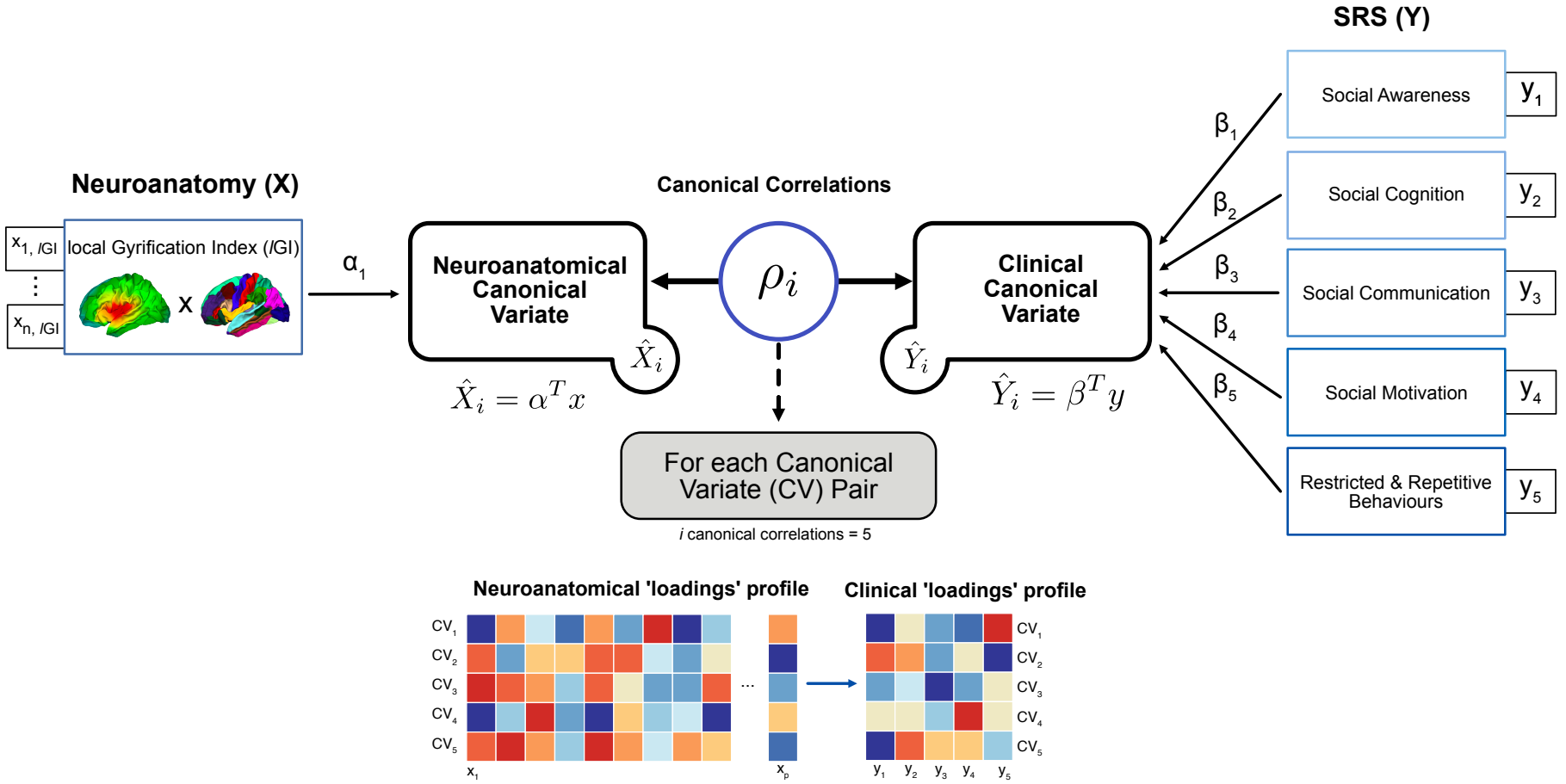

CCA was used to examine the relationship between neuroanatomical variability in regional local gyrification index (lGI) as predictor (X; left panel), and the five Social Responsiveness Scale (SRS) subdomain scores in (1) social awareness (SAW), (2) social cognition (SCG), (3) social communication (SCM), (4) social motivation (SM), and (5) restricted and repetitive behaviors (RRB) as clinical outcomes (Y; right panel). CCA estimates two parameter ectors α and β so that the correlation ρ between the linear combinations $\hat{X} = \alpha^T X$ and $\hat{Y} = \beta^T Y$ is maximised. The resulting predicted variables $\hat{X}_1$ and $\hat{Y}_1$ are the first pair of canonical variates (*CV*s), and their correlation ρ_1 is the first canonical correlation *(CC)*. The 2nd set of parameter estimates maximising ρ is then derived subject to the constraint of being uncorrelated with the first pair of canonical variates. This procedure may be continued up to i times, where $i = \min\{p, q\}$, resulting in maximally i canonical variate pairs.

S7 - Cluster information

Clusters with significantly increased and decreased local Gyrification Index (lGI) for the main effect of 22q11.2DS

Cluster	Regional Labels	Side	BA	Vertices	t_{max}	p	Talairach coordinates x y z
Main Effect 22q11.2DS							
1	Insula, pars opercularis, postcentral gyrus, precentral, superior temporal gyrus	R	6, 21-22, 38-43	9647	4.20	$1.63*10^{-5}$	57 0 -7
2	Insula, middle temporal gyrus, pars opercularis, postcentral gyrus, precentral, superior temporal gyrus, transverse temporal cortex	L	4-6, 21-22, 38-40, 43-44, 52	10175	4.48	$1.63*10^{-5}$	-58 -9 -21
3	Fusiform gyrus, parahippocampal gyrus	R	20, 35-37	1705	3.59	$1.64*10^{-5}$	23 -15 -25
4	Superior temporal gyrus	L	41-42	1386	3.08	$3.47*10^{-3}$	-64 -26 3
5	Caudal anterior-cingulate cortex, caudal middle frontal gyrus, cuneus cortex, inferior parietal cortex, isthmus-cingulate cortex, lingual gyrus, medial orbital frontal cortex, paracentral lobule, pericalcarine cortex, postcentral gyrus, posterior-cingulate cortex, precentral gyrus, precuneus cortex, rostral anterior cingulate cortex, superior frontal gyrus, superior parietal cortex, supramarginal gyrus	R	1-6, 8-11, 17-19, 23-27, 29-33	48089	-1.66	$1.63*10^{-5}$	6 -53 19
6	Caudal anterior-cingulate cortex, cuneus cortex, fusiform gyrus, isthmus-cingulate cortex, lateral orbital frontal cortex, lingual gyrus, medial orbital frontal cortex, paracentral lobule, pericalcarine cortex, posterior-cingulate cortex, precuneus cortex, rostral anterior cingulate cortex, superior frontal gyrus, superior parietal cortex	L	1-6, 8-11, 17-19, 23-27, 29-33	27955	-1.66	$1.63*10^{-5}$	-11 -66 12
7	Postcentral gyrus, precentral gyrus, superior parietal cortex, supramarginal gyrus	L	1-4, 7	9017	-1.66	$1.63*10^{-5}$	-29 -24 46
8	Uncus	R	28	66	-1.66	$2.08*10^{-4}$	25 -7 -26
9	Middle temporal gyrus	R	20-21	1190	-1.66	$1.11*10^{-3}$	58 -40 -9
10	Middle frontal gyrus	R	19	1406	-1.66	$1.91*10^{-3}$	40 40 18

Note: Side: L: Left, R: Right; BA: approximate Brodmann area(s); Vertices: number of vertices within the cluster; tmax: maximum t-statistic within the cluster; p: cluster-corrected p-value

Clusters with significantly increased and decreased local Gyrification Index (lGI) for the main effect of ASD and 22q11.2DS-by-ASD interaction effect

Cluster	Regional Labels	Side	BA	Vertices	t_{max}	*p*	Talairach coordinates x y z
Main Effect ASD							
1	Precentral gyrus	R	6	2390	3.53	$1.87*10^{-5}$	56 7 26
2	Entorhinal cortex, fusiform gyrus	L	28, 34-37	871	3.89	$5.09*10^{-5}$	-20 -17 -21
3	Parahippocampal gyrus	L	27-28	182	5.31	$1.98*10^{-4}$	-12 -43 5
4	Superior frontal gyrus	L	6	1136	3.41	$7.34*10^{-4}$	-19 11 55
5	Posterior cingulate cortex	R	29	97	3.30	$3.60*10^{-2}$	11 -44 6
6	Uncus	L	28	46	4.10	-1.72	-25 -9 -25
7	Middle Temporal gyrus	L	21-22	1156	4.72	-1.65	-58 -10 -20
Interaction Effect 22q11.2DS * ASD							
1	Insula, pars triangularis	R	45, 52	2352	3.02	$1.65*10^{-5}$	29 21 5
2	Precentral gyrus, postcentral gyrus,	L	1-4	2405	2.79	$4.21*10^{-5}$	-33 -27 51
3	Parahippocampal	L	35	33	3.46	$3.62*10^{-2}$	-22 -13 -23
4	Postcentral gyrus, superior parietal cortex	L	4-5, 7	1171	3.60	$4.33*10^{-2}$	-21 -39 56
5	Postcentral gyrus, supramarginal gyrus	R	40, 43	3120	-1.66	$1.74*10^{-5}$	62 -34 16
6	Parahippocampal	L	30	258	-1.66	$3.45*10^{-5}$	-12 -43 5
7	Inferior temporal gyrus, middle temporal gyrus	R	20-21	1176	-1.66	$1.41*10^{-4}$	59 -43 -5
8	Supramarginal gyrus	L	4, 40, 43	1182	-1.66	$1.43*10^{-3}$	-61 -29 25
9	Inferior parietal cortex, lateral occipital cortex, superior parietal cortex	L	18-19	2214	-1.66	$3.77*10^{-3}$	-37 -79 25
10	Rostral middle frontal cortex	R	9-10, 46	1359	-1.66	$4.26*10^{-3}$	39 35 23

Note: Side: L: Left, R: Right; BA: approximate Brodmann area(s); Vertices: number of vertices within the cluster; tmax: maximum t-statistic within the cluster; p: cluster-corrected p-value

S8 - Distribution of mean *l*GI across groups in interaction

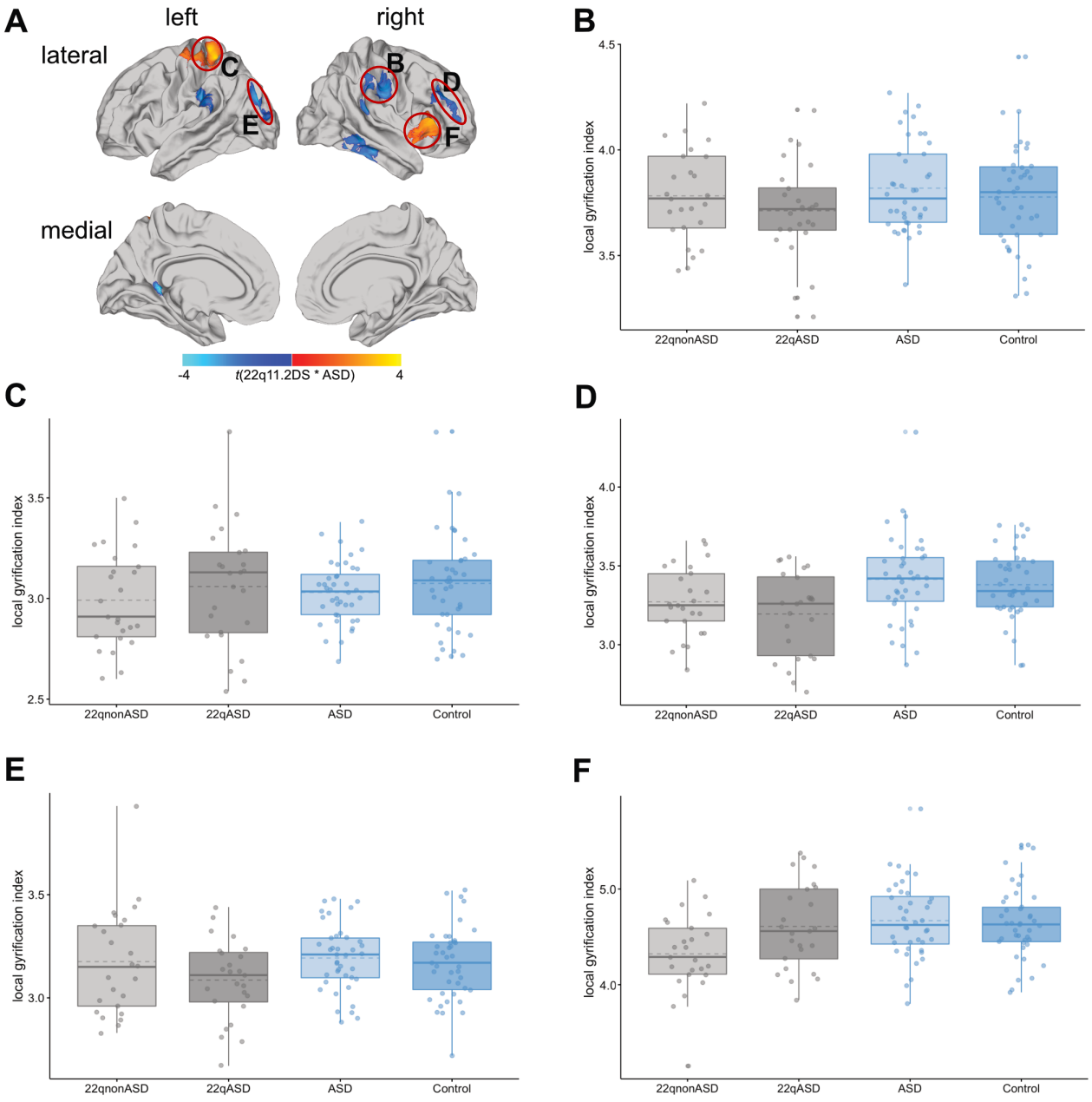

Figure S8. (A) Clusters with significant 22q11.2DS-by-ASD interaction effects for local gyrification index (*l*GI), where letters next to each cluster refer to the corresponding sub-plots. Here, solid bars indicate median values of each group, with lower and upper hinges corresponding to the first (25th percentile) and third (75th percentile) quartiles. Dashed bars indicate mean values. Variability in lGI across the four groups in (B) right postcentral and supramarginal gyri, (C) left superior parietal cortex and postcentral gyrus, (D) right rostral middle frontal cortex, and (E) left superior and inferior parietal cortex, and lateral occipital cortex, and (F) right insula and pars triangularis.

S9 - Results of the Categorical Analysis after covarying for repetitive symptoms.

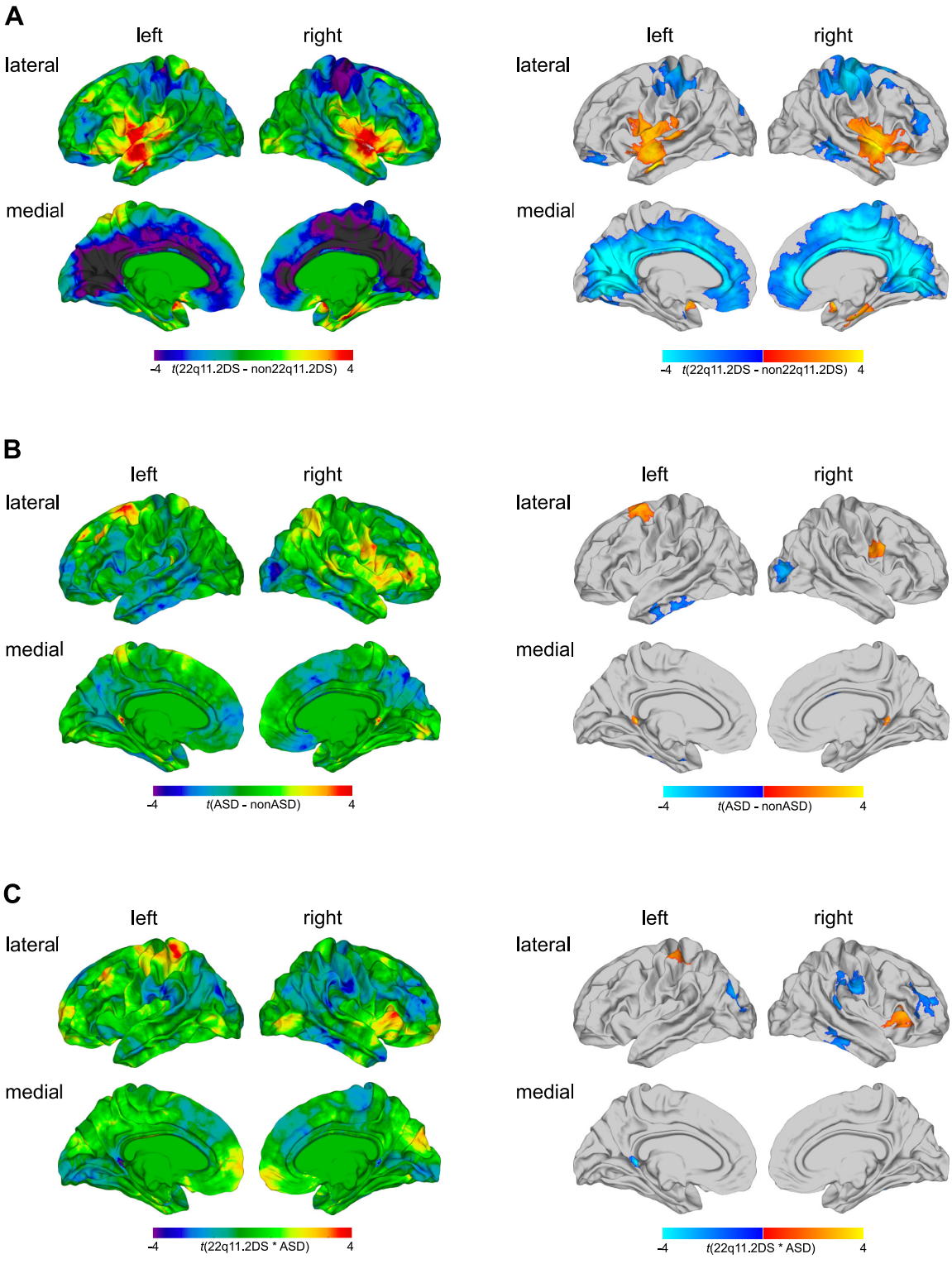

Figure S9. Significant differences in local gyrification for (A) the main effect of 22q11.2DS, (B) the main effect of ASD, and (C) the 22q11.2DS-by-ASD interaction effect when covarying for interindividual differences in repetitive symptoms. Displayed are both the unthresholded t-maps (left panel) and the random field theory (RFT)-based cluster corrected ($p<0.05$, 2-tailed) t-maps (right panel). Here, increased parameter estimates in 22q11.2DS or ASD relative to their respective counterparts are marked in red to yellow, and decreased parameters are marked in blue to cyan.

S10 - Neuroanatomical loadings

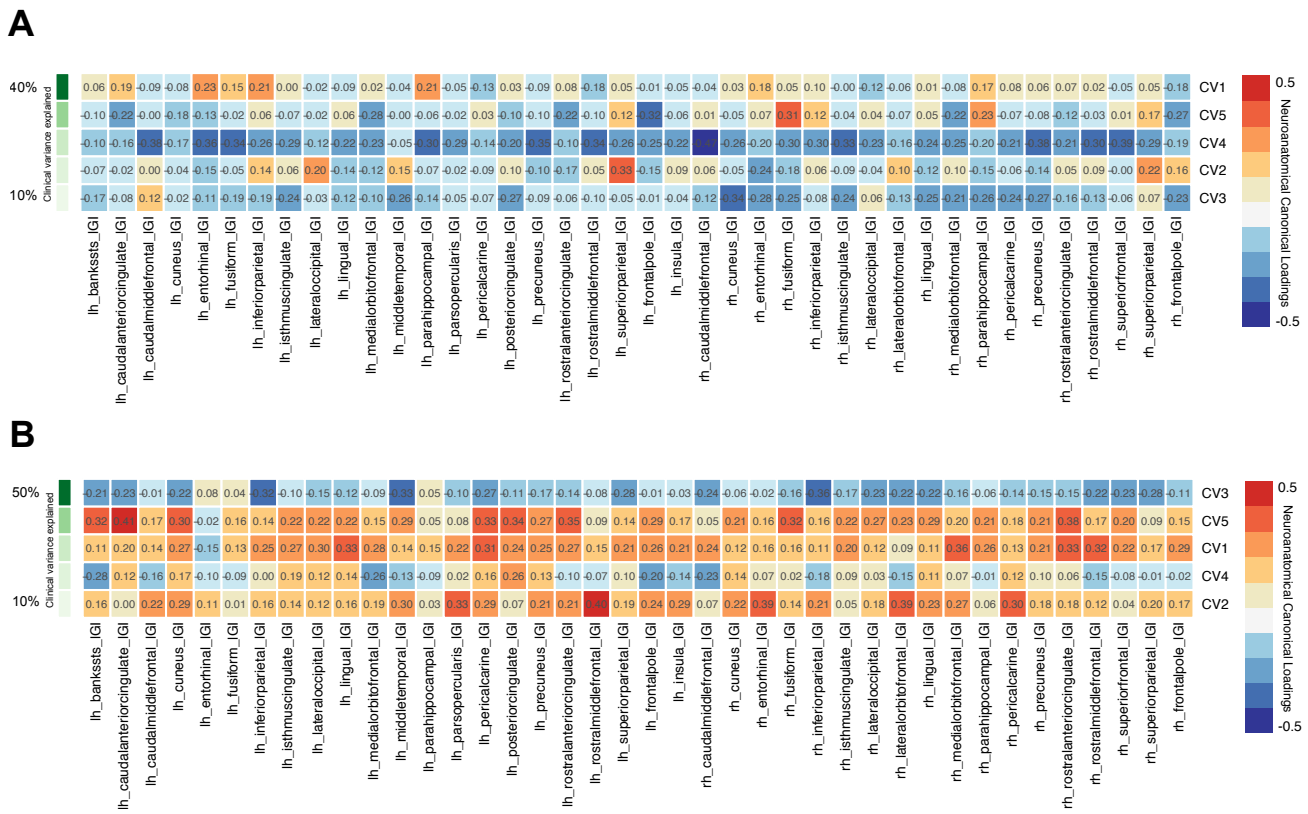

Figure S10. Neuroanatomical loading plots illustrating the neuroanatomical canonical loadings (i.e. correlations) between measures of the local gyrification index (*l*GI) in the set of 40 ROIs with the respective five neuroanatomical canonical variates (CVs) within the individuals without the 22q11.2 microdeletion; (B) and within individuals with the 22q11.2 microdeletion. CVs are sorted in descending order based on the percentage of clinical variance explained, indicated in shades of green on the left.

References:

Döpfner M, Lehmkuhl G, Görtz-Dorten A, Breuer D. 2008. DISYPS-II : Diagnostik-System für psychische Störungen nach ICD-10 und DSM-IV für Kinder und Jugendliche - II. Bern: Huber : Hogrefe Testverl.

First MB, Gibbon M. 2004. The Structured Clinical Interview for DSM-IV Axis I Disorders (SCID-I) and the Structured Clinical Interview for DSM-IV Axis II Disorders (SCID-II). In. Comprehensive handbook of psychological assessment, Vol. 2: Personality assessment. Hoboken, NJ, US: John Wiley & Sons Inc p 134-143.

Gotham K, Pickles A, Lord C. 2009. Standardizing ADOS Scores for a Measure of Severity in Autism Spectrum Disorders. J Autism Dev Disord. 39:693-705.

Gudbrandsen M, Daly E, Murphy CM, Wichers RH, Stoencheva V, Perry E, Andrews D, Blackmore CE, Rogdaki M, Kushan L, Bearden CE, Murphy DGM, Craig MC, Ecker C. 2019. The Neuroanatomy of Autism Spectrum Disorder Symptomatology in 22q11.2 Deletion Syndrome. Cereb Cortex. 29:3655-3665.

Hus V, Gotham K, Lord C. 2014. Standardizing ADOS Domain Scores: Separating Severity of Social Affect and Restricted and Repetitive Behaviors. J Autism Dev Disord. 44:2400-2412.

McGlashan TH. 2001. Structured Interview for Prodromal Syndromes (SIPS). New Haven: Yale University.

Shaffer D, Schwab-Stone M, Fisher P, Cohen P, Placentini J, Davies M, Conners CK, Regier D. 1993. The Diagnostic Interview Schedule for Children-Revised Version (DISC-R): I. Preparation, Field Testing, Interrater Reliability, and Acceptability. Journal of the American Academy of Child & Adolescent Psychiatry. 32:643-650.